STUDY OF ELEMENTARY MICRO-CUTTING IN HARDENED TOOL STEEL

R. Piquard[1]*, A. Gilbin[1], M. Fontaine[1], A. D'Acunto[2], S. Thibaud[1], D. Dudzinski[2]

[1]FEMTO-ST UMR 6174, CNRS/UFC/ENSMM/UTBM, Dépt Mécanique Appl., Besançon, France

[2]LEM3 UMR 7239, Université de Lorraine, Arts et Métiers ParisTech, CNRS, ENIM, Metz, France

*Corresponding author; e-mail: romain.piquard@femto-st.fr

Abstract

In order to model micro-milling cutting forces, a way is to apply a local model on discretized elements of the cutting edge and then summing on the whole edge to obtain the global cutting forces. This local model is usually obtained by numerical simulation or cutting experimentation. This paper focuses on orthogonal and oblique micro-cutting experiments of AISI 6F7 with tungsten carbide tools. Results show the influence of cutting edge sharpness on cutting forces and the existence of different mechanisms corresponding to different ranges of uncut chip thickness values. A phenomenological model has been identified to model correctly these zones. Then, by comparing experimental micro-milling forces with those deduced from these micro-cutting model and tests, a good agreement has been found. In order to complete this study, phenomenological and thermo mechanical models are being developed. The aim is to obtain an elementary cutting model that can be used for micro-milling simulation and optimization.

Keywords:

Micro-cutting; micro-milling; experimentation; simulation; hardened tool steel

1 INTRODUCTION

Studying micro-machining and in particular micro-milling is quite new compared to the conventional machining. Micro-milling is mainly characterized by tools having a diameter less than 1 mm and that can reach 0.05 mm. These tools do not have complex geometries and proportional sharpness of conventional tools because of the difficulty in manufacturing by abrasion such small parts. With these small tools, cutting parameters are also very different from conventional machining, it is recommended to use "adapted" conditions related to the diameter: thus, it is possible to achieve depths of cut and feed per tooth of a few microns and spindle speeds above 100 000 rpm in order to obtain sufficient cutting speeds. However, the "top-down" approach used in micro-milling consisting in proportionally downsizing the conventional milling parameters reaches to the appearance of size effects. The size effect is defined as a divergence of values of characteristic parameters from theoretical values at a reference scale. For instance cutting edge sharpness (also called cutting edge radius to uncut chip thickness ratio) is more critical in micro-milling milling than in conventional milling.

These size effects are relevant issues in understanding the mechanisms of micro-cutting and are the issues of most of the scientific studies conducted on micro-cutting including the study of cutting forces. However, most of these studies apply a force model directly to the case of micro-milling process which can cause difficulties to distinguish and identify dynamical, geometrical and structural effects from

cutting forces and surface roughness analysis. For instance Bissacco et al. [Bissacco 2008] proposed a model based on the unified mechanics of cutting approach proposed by Armarego, but adapted to micro-milling and taking into account the tool run-out measured on the machine, theoretically leading to different loads, and thus to different forces, on each tooth. Cutting forces measured during experiments did not show this distinctive feature, probably as a result of tool bending, dividing forces on each tooth. Thus a purely geometrical model is difficult to use.

Concerning orthogonal cutting models, most came from numerical results of cutting simulation. Altintas and Jin [Altintas 2011] modeled the cutting forces as a function of uncut chip thickness h and cutting edge radius r_β as shown in equation (1).

$$F_{t,f} = K_{t,f}(h, r_\beta)hw = (\alpha_{t,f}h^{d_{t,f}} + \beta_{t,f}h^{p_{t,f}}r_\beta^{q_{t,f}})hw \quad (1)$$

The coefficients $\alpha_i, \beta_i, d_i, p_i$ and q_i were constants. Forces were thus directly related to the specific cutting force K_i and uncut chip section.

Afazov et al. [Afazov 2010] proposed a modeling dependent on cutting speed given in equation (2).

$$F_{c,t} = (p_1 v_c^{p_2})[1 - e^{p_3 h}] + (p_4 v_c + p_5)[1 - e^{p_6 h}] \quad (2)$$

The coefficients p_i were also constant. This model did not involve cutting edge radius which was in fact taken into account in tool geometry used in the simulation.

These models shown that the cutting forces are not linear functions of uncut chip thickness but increase rapidly at low uncut chip thicknesses to stabilize to a more linear model

demonstrating the influence of cutting edge radius for a h/r_β ratio close to 1.

2 EXPERIMENTAL SETUP

A solution to avoid such dynamical issues and to focus on local material deformation is to consider a simpler case, namely the elementary micro-cutting. In this case the assumption of a rigid tool is suitable and cutting process is continuous through the overall experiment. Thus it is easier to define a model taking into account only geometrical aspects. Then this model can be applied to the case of the micro-milling by geometric transformation and expanded to take into account precisely other effects, such as dynamic effects.

Micro-cutting tests have to be carried out. This can be done in several ways: by planing, by turning a disk or a tube. Planing corresponds directly to the elementary cutting configuration but can be limited in cutting speed which is in this case the displacement speed of linear axis. The two other cases can be performed using a spindle and permit to reach higher cutting speed even if some assumptions have to be made on the homogeneity of velocity and deformation. In this study, turning of a tube was chosen in order to use the high velocity and rigidity of a CNC classically devoted to High-Speed Machining. A phenomenological model has been deduced from the obtained results, taking into account the cutting edge sharpness through an equivalent cutting edge radius.

2.1 Experimental micro-cutting procedure

A CNC Röders RP600 was used to turn a tube disposed in the spindle. This tube was turned first directly on the experimental bench, shown on figure 1, to obtain the desired cutting width and a limited workpiece run-out. Cutting conditions for experiments are defined according to the technological limitations of this milling machine, such as a feed speed value that could only be an integer value.

In addition to these limitations, the assumptions of micro-cutting must be taken into account: the uncut chip thickness must be small compared to the width of cut to be able to neglect the boundary effects, and the width should not be too large to consider a constant cutting speed along the cutting edge.

Fig 1: Micro-cutting experimental setup

Knowing all these limits, the dimensions used for the tube is an average diameter of 6.366 mm and a thickness of 318 µm. This thickness is calculated for a speed variation along the cutting edge inferior to 10% and an uncut chip thickness limited to 31 microns.

The forces are measured using a multicomponent dynamometer Kistler Minidyn 9256 C2. The tool is fixed on this dynamometer, leading to constant measured forces through experiment. The measured forces F_x, F_y and F_z are directly the forces of tool on material in orthogonal cutting with the y direction aligned with the cutting edge.

Such forces were obtained in the dynamometer reference system and a geometrical transformation was used to obtain the force components F_c, F_p and F_f applied to the workpiece in the tool reference system in the case of oblique cutting as shown on Fig. 3. In addition, the offset and linear divergence of the measured signal was identified and subtracted in order to have a zero value when the tool was not cutting.
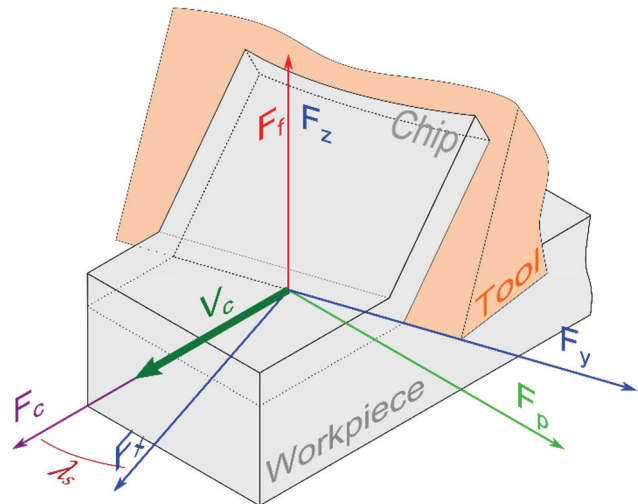

Fig 2: Considered cutting forces in oblique cutting tests

2.2 Cutting conditions and work material

The tests presented here were performed on an AISI 6F7 steel (40NiCrMo16) hardened to54 HRC. This steel is classically used in tooling for injection moulding. Concerning cutting conditions, a cutting speed of 60 m/min (3000 rpm) was used, uncut chip thickness was set between 0.165 µm and 12 µm. Two rake angles (-8° and 8°) were tested in orthogonal cutting as well as in oblique cutting (λ_s = 30°). Equivalent cutting edge radius of these tools (IFANGER MTNY-41015-R TiAlN coated) were measured using a topo-microscope Alicona Infinite Focus (X100 lens) and an average value of 1.3 µm has been found.

In order to compare micro-cutting with micro-milling, some slots were machined in the same material with a two flutes flat micro-end mill with a diameter of 0.5 mm and without helix angle. The same cutting speed of 60 m/min was used, leading to a spindle speed of 38197 rpm. Three values of axial engagement (20 µm, 40 µm and 60 µm), and three values for feed per tooth (1 µm, 5 µm and 10 µm) were used. The tests were performed on an AgieCharmilles 5 axis CNC MIKRON HSM400U LP.

3 RESULTS AND DISCUSSION

By observing the plots presenting forces as a function of uncut chip thickness (Figure 3), we notice a fast increase of forces to lower thicknesses for all cutting configurations. This observed jump is probably due to the combined action of a change in material solicitation and local hardening. Local hardening has been observed in conventional milling of AISI 6F7 as has shown in Fig. 4 (V_c = 125 m/min, f_z = 0.1 mm, a_p = 0.5 mm, tool: Sandvik 345R-1350E-PL 1010) Indeed, under the action of ploughing effect at small

thickness, specimen is hardened during the previous path of the tool and cutting forces increase when the tool attempts to cut into this zone.
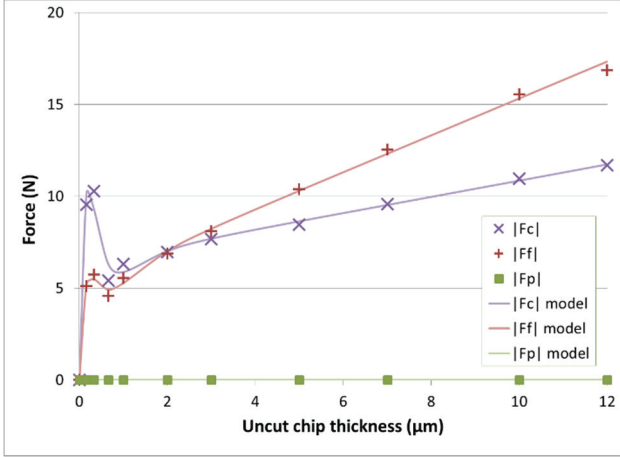

Fig 3: Cutting forces as a function of uncut chip thickness

As the test is cyclical (several rotations in an experiment), the phenomenon is added at each rotation and is more pronounced when the uncut chip thickness is smaller than the thickness hardened. On the contrary if the thickness of the chip is larger, the hardened surface of the previous rotation is removed by chip formation and a new hardened surface appears, the accumulation does not take place. This phenomenon has already been observed in AISI 1045 by Fleischer et al. [Fleischer 2009] for a ratio r_β/h close to 1.
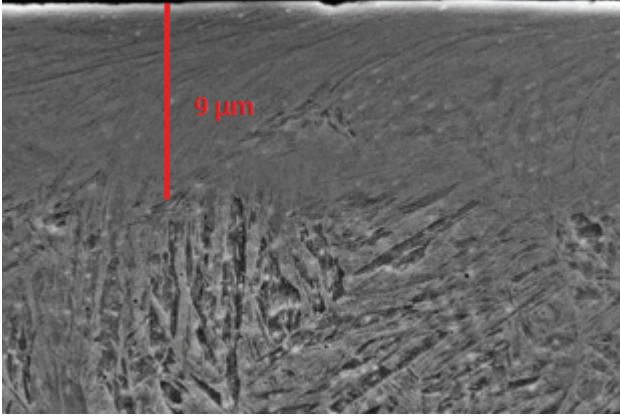

Fig. 4: Hardening observed in conventional milling

To take into account this jump into a phenomenological model, it is proposed that this model is decomposed into two terms: the first has to be valid at small thicknesses, the second has to be valid at larger thicknesses. The proposed model is given in equation (3).

$$F = K_1.h\left(e^{-\frac{\alpha_1 h}{r_\beta}}\right) + (K_2.h + K_3).\left(1 - e^{-\frac{\alpha_2 h}{r_\beta}}\right) \quad (3)$$

The coefficients K_i and α_i are constants and depend on machined material and tool geometry. The first term is a linear function weighted by a factor of saturation which tends to 0 as thickness increases. This term may be the representation of the cutting edge radius effect. The second term is an affine function weighted by a factor that is null when thickness is also null, and tends to 1 when thickness is increasing. Then the jump represents the transition between the two terms.

MIC2M [Richard 1999] is a software developed on MATLAB for parameter identification from the Levenberg Marquardt or a genetic algorithms. A module has been implemented

on MATLAB and has been included in MIC2M for identifying different coefficients directly from the results of micro-cutting experiments. The cutting forces coefficients in cutting speed direction F_c, in a direction orthogonal to the machined surface F_f and in a direction orthogonal to the two previous directions F_p (see figure 2) are given respectively in Tab. 1 a), b) and c).

Tab 1: Cutting force coefficients

a) F_c	Rake angle γ = 8°		Rake angle γ = -8°	
Coefficients	λ_s = 0°	λ_s = 30°	λ_s = 0°	λ_s = 30°
K_1	59,78	56,25	4148,17	139,53
α_1	-11,09	-11,49	-84,33	-24,81
K_2	1,00	1,08	1,83	1,60
K_3	5,28	5,36	5,22	7,48
α_2	-3,24	-4,54	-5816,59	-6,63

b) F_f	Rake angle γ = 8°		Rake angle γ = -8°	
Coefficients	λ_s = 0°	λ_s = 30°	λ_s = 0°	λ_s = 30°
K_1	137,96	132,70	138,00	72,98
α_1	-11,67	-12,30	-16,00	-16,28
K_2	0,44	0,54	1,46	1,44
K_3	6,43	6,11	6,91	8,35
α_2	-3,18	-5,94	-332,00	-332,43

c) F_p	Rake angle γ = 8°		Rake angle γ = -8°	
Coefficients	λ_s = 0°	λ_s = 30°	λ_s = 0°	λ_s = 30°
K_1	0	5,07	0	2,93
α_1	0	-11,08	0	-6,18
K_2	0	-0,28	0	-0,35
K_3	0	-0,18	0	-0,03
α_2	0	-1941,8	0	-6,18

It may be noted that the coefficient K_1 is more important for the tool with a negative rake angle, which can be a sign of a cut refusal larger than the tool with positive rake angle. Moreover, for the tool with a positive rake angle, the coefficients are not influenced by the inclination angle leading to the same model in orthogonal and oblique cutting.

3.1 Micro-cutting simulation

The experiments also permitted to find some material parameters needed for the implementation of a numerical simulation. A first point is the identification of the friction angle. According to the Merchant model [Merchant 1945], the ratio between normal force F_t and cutting force F_c is only related to rake angle and friction angle in orthogonal cutting conditions as shown in equation (4).

$$\frac{F_f}{F_c} = \tan(\mu - \alpha) \quad (4)$$

Thus, it is possible to obtain the friction angle μ by knowing forces and nominal rake angle (equation (5)).

$$\mu = \alpha + \arctan\frac{F_f}{F_c} \quad (5)$$

By plotting the coefficient of friction according to the uncut chip thickness for the two nominal rake angles of 8° and -8° in orthogonal cutting, the limits of the Merchant model considering a perfectly sharp cutting edge (no cutting edge radius) is underlined (Fig. 5).
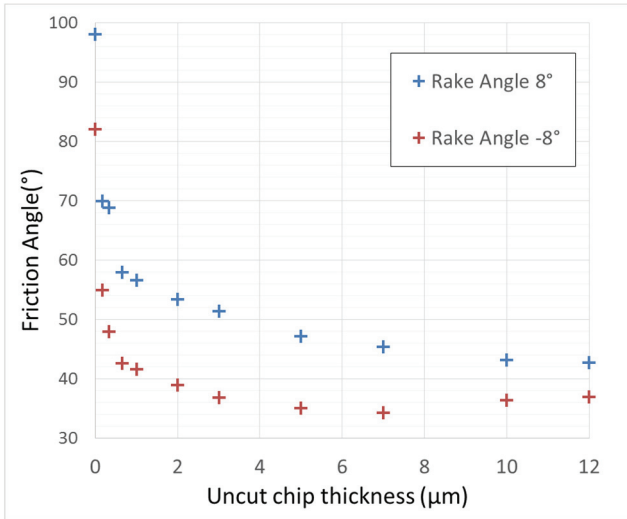
Fig. 5: Nominal friction angle as a function of uncut chip thickness

The friction coefficient shows a decreasing evolution as uncut chip thickness increases which highlights the fact that the effective cutting angle diverges from the nominal angle for the smaller thicknesses. Nevertheless the friction angle converges to a constant value of about 40° corresponding to a friction coefficient of 0.84. Lower values for the negative rake angle compared to those for the positive angle can be explained by an additive force depending on rake angle. Ploughing can be an explanation which has less influence at higher thicknesses reaching to values convergence.

The numerical simulation has been implemented in LS-DYNA using smoothed particle hydrodynamics method (SPH) in explicit formulation (Fig. 6). A Johnson-Cook constitutive law is used to model machined material behaviour. About 24 h are necessary to simulate a cutting distance of 0.1 mm.

The first results of numerical simulations performed considering the behaviour of a material close to AISI 6F7 appear to be consistent with the observations made during experimental tests, but do not show the same force jump, reinforcing the assumption of accumulated hardening during the experimentation which was not simulated.
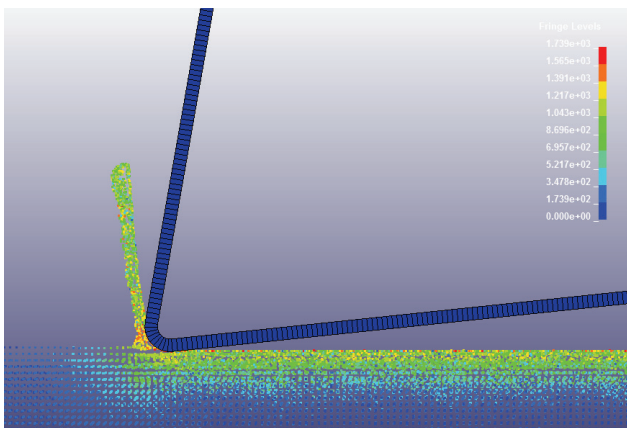

Fig 6: Example of a SPH micro-cutting simulation

3.2 Comparison with micro-milling

In order to apply the model to micro-milling, the method of edge discretization is used. This method consists to apply a local model on every small part of the cutting edge and then summing all the elementary forces of every edge part. The algorithm is based on a milling parametric model previously developed [Fontaine 2007] by modifying only the expression of the local elementary cutting model by the cutting model given in equation (3). This algorithm has been implemented in the software MIC2M in a previous work dealing with high speed milling. Direct simulation without identification and without taking into account dynamical considerations gives interesting results as can be seen in Fig 7. The coefficients used are those which have been identified for micro-cutting (given in Tab. 1). This figure shows experimental values as a function of model values which have to be the closest to the bisecting line as an indicator of a good simulation. The plotted values are the mean values of cutting forces as well as amplitude values. It can be seen that some values show a good agreement between experiment and simulation and worst agreement for small and high values.
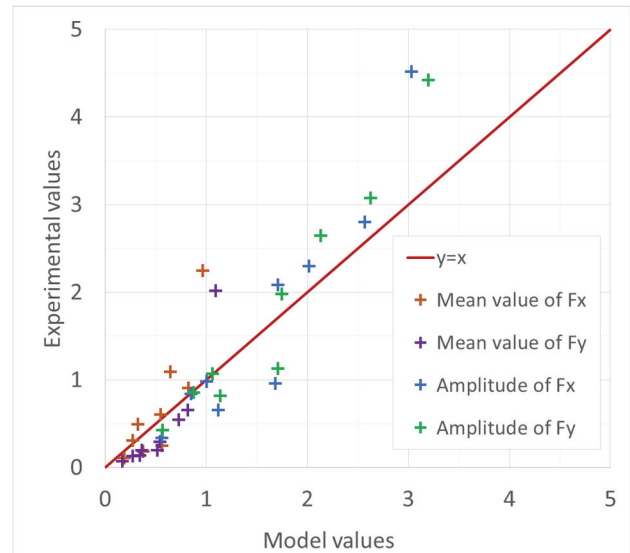

Fig 7: Comparison of model and experimental values

The best simulation is for a feed per tooth f_z equals to 5 μm and for an axial engagement a_p of 60 μm. The corresponding cutting forces are given in Fig 8 with cutting forces in the direction perpendicular to the feed F_x and in the direction of the feed F_y on two rotations (i.e. four tooth passes). In addition to the mean value and amplitude value, a good agreement with the shape of cutting signal is also notable. A small difference between the experimental cutting forces of the teeth is observable on F_x and F_y and is mainly due to the tool run-out which is not informed in the model.
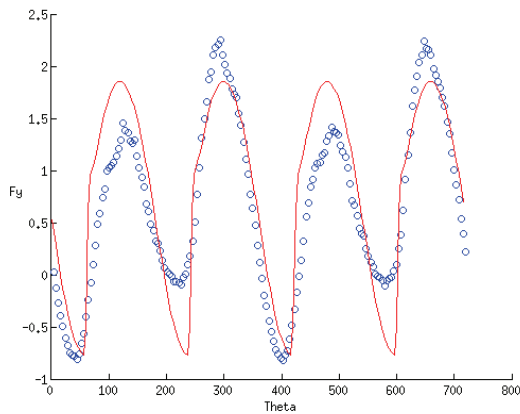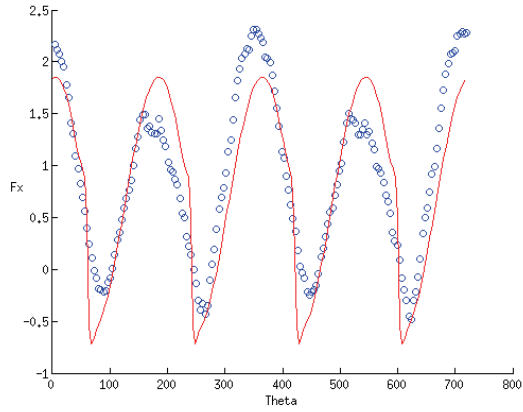
Fig 8: Cutting forces from model (continuous line) and experiments (dots) for f_z = 5 µm and a_p = 60 µm

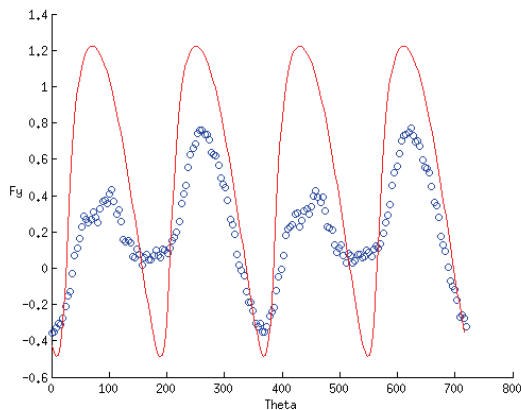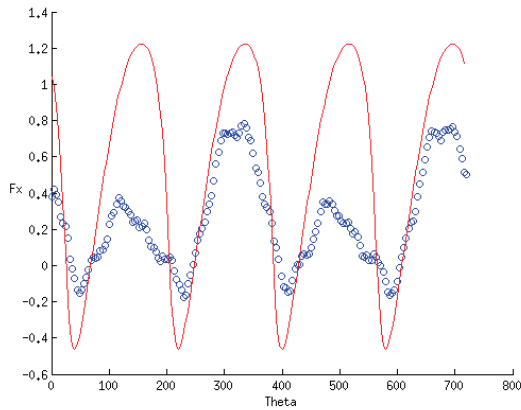*Fig. 9: Cutting forces of model (continuous line) and experiment (dots) for f_z = 1 µm and a_p = 60 µm*

The worst simulation (biggest relative error) is for a feed per tooth f_z equals to 1 µm and for an axial engagement a_p of 60 µm. The corresponding cutting forces are given in Fig 9. The shape of force signal is largely different between experimental results and model. Experimental results show pointed peaks for the less loaded tooth and that can be explained by a cutting refusal associated to a tool deflection.

The run-out effect is clearly observable. This default can be measured statically and informed in the model to obtain adjusted curves but it is not the only factor of discrepancy. For larger feed per tooth, the difference of mean values can be a result of tool deflection that adds a static value on forces. This can be modelled as a beam deflection which can be implemented in the micro-milling model.

Another comparison has been made between micro-cutting coefficients identified from micro-milling tests performed in previous work [Gilbin 2012] and from micro-cutting tests as described in section 2. The used elementary cutting law and cutting edge radius are slightly different but the results are really interesting to compare. On the top of Fig 9, one can see specific cutting forces K_ψ and K_r corresponding respectively to tangential and radial directions of the micro end mill. The expression of these coefficients is given in equation (6).

$$K = K_1 e^{\alpha_1\, f_z/f_0} + K_2 e^{\alpha_2\, f_z/f_0} \qquad (6)$$

The second chart shows specific cutting forces K_c and K_f corresponding respectively to the cutting direction and an orthogonal direction to the machined surface for micro-cutting. Thus according to the micro end mill geometry, K_ψ and K_r are equivalent to K_c and K_f respectively. Each chart show a cross between the two curves for a feed per tooth and an uncut chip thickness close to the cutting edge radius value. This correspond to a ploughing dominant regime for the lowest values of thicknesses. It can be noticed that K_r and K_f curves are quite similar and reach the same value (about 2500 MPa) when thickness increases. Concerning K_ψ and K_c, the trends are different with a lower slope for K_ψ which can be due to flexibility of the tool and a cutting refusal when the uncut chip thickness is equivalent to the cutting edge radius. Moreover, the tool sharpness is lesser for the milling tests and it probably participates to this form discrepancy. This comparison reinforces the idea that micro-milling cutting forces can be predicted thanks to elementary micro-cutting experiments and dynamical considerations.
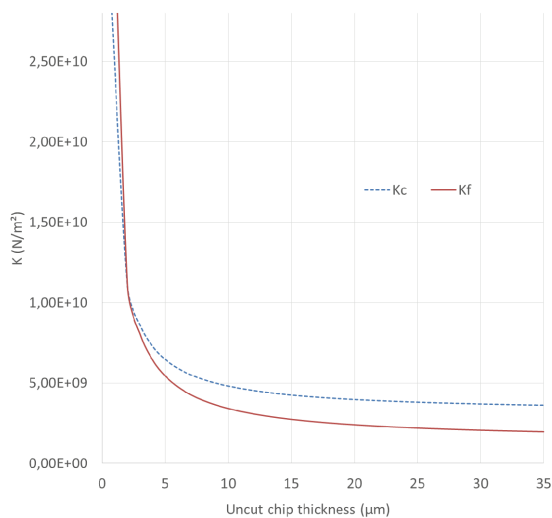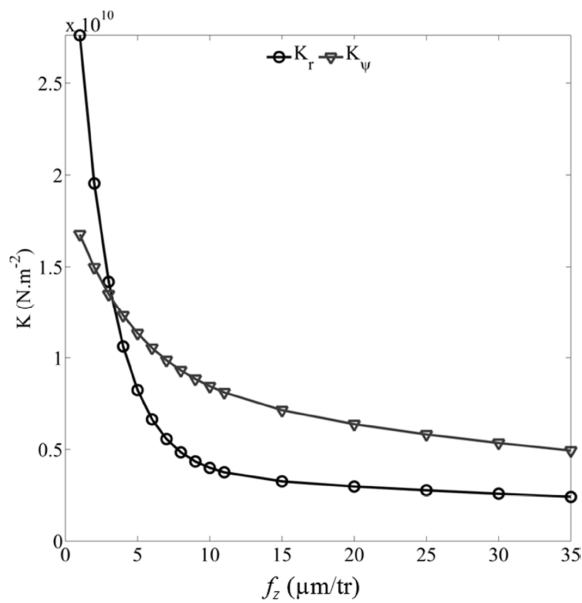
Fig. 9: Comparison of identified specific cutting forces between micro-milling (top) and elementary micro-cutting model (bottom)

4 CONCLUSION

This work focuses especially on elementary micro-cutting experimentation based on turning. This permits to emphasis cutting edge radius effect (or sharpness defects) on cutting forces for low uncut chip thicknesses. An important ploughing effect has been observed for the lowest values of thickness. This elementary micro-cutting experimentation will be used for validation of numerical simulations using LS-DYNA. Then, micro-milling cutting forces will be easily predicted with appropriate cutting law and more information will be available to analyse phenomena inherent to micro-cutting and to validate the identification of cutting laws directly performed from micro-milling tests In order to propose a precise prediction of cutting forces in micro-milling, dynamical effects have to be taken into account in used milling model and MIC2M software.

Concerning numerical modelling, a simulation of micro-cutting on tube turning is being studied which has a high computational cost due to a large number of nodes, but aims to fill the gap between experimentation and numerical simulation of elementary micro-cutting. Mechanical tests have to be performed on the machined material to find the suitable parameters of the Johnson-Cook constitutive law in the range of machining conditions.

6 REFERENCES

[Afazov 2010] Afazov, S.M., Ratchev, S.M. and Segal, J., Modelling and simulation of micro-milling cutting forces. Journal of Materials Processing Technology. 2010. Vol. 210, n° 15, pp. 2154‑2162. DOI 10.1016/ j.jmatprotec.2010.07.033.

[Altintas 2011] Altintas, Y. and Jin, X., Mechanics of micro-milling with round edge tools. CIRP Annals-Manufacturing Technology. 2011. Vol. 60, n° 1, pp. 77–80.

[Bissacco 2008] Bissacco, G., Hansen, H.N. and Slunsky, J., Modelling the cutting edge radius size effect for force prediction in micro milling. CIRP Annals - Manufacturing Technology. 2008. Vol. 57, n° 1, pp. 113‑116. DOI 10.1016/j.cirp.2008.03.085.

[Fleisher 2009] Fleisher, J., Schulze, V. and Kotshenreuter, J., Extension of cutting force formulae for microcutting. CIRP Journal of Manufacturing Science and Technology. 2009. Vol. 2, n° 1, pp. 75–80.

[Fontaine 2007] Fontaine, M., Devillez, A. and Dudzinski, D., Parametric geometry for modelling of milling operations. International Journal of Machining and Machinability of Materials. 2007. Vol. 2, n° 2, pp. 186–205.

[Gilbin 2012] Gilbin, A., Influence of feed rate in micro-milling studied from experiments and micro-cutting laws identification. Proceedings of the 8th International Conference on MicroManufacturing. 2013.

[Merchant 1945] Merchant, ME, Mechanics of the metal cutting process. American Institute of Physics. 1945.

[Richard 1999] Richard, F., http://mic2m.univ-fcomte.fr/, 1999